

Robust one-step (deconvolution + integration) seismic inversion in the frequency domain

Ivan Priezzhev* and Aaron Scollard, Schlumberger

Summary

Seismic inversion requires two main operations relative to changes in the frequency spectrum. The first operation is deconvolution, used to increase the high frequency component of the observed seismic data and the second operation is integration of a reflectivity function to decrease the high frequencies and increase low frequencies of the seismic signal. The first operation is very unstable and non-unique for noisy seismic data. The second operation is very stable in high frequencies but has problems in low frequencies due to undefined low frequency data in seismic traces. By performing both of these operations simultaneously the operation will be stable in high frequency area and can be effectively stabilized in low frequency area based on an a priori acoustic impedance power spectrum and use Tikhonov and Arsenin's (1979) regularization technique. This approach can be applied to post-stack and pre-stack seismic data.

Introduction

Seismic inversion is an important processing step in reservoir characterization that allows property prediction, away from the well control, as it may be used to compute acoustic impedance from poststack data, and p- and s-wave velocity, plus density, from prestack data. The results can be used, for instance, as 3D trends for petrophysical or facies modeling. Most seismic inversion techniques use two steps to calculate acoustic impedance. The first step is deconvolution and the second step is integration. Deconvolution operation is very unstable because it creates a set of unlimited-frequency reflection coefficients from a frequency-limited seismic trace. Many deconvolution and inversion technologies use sparse signal theory to perform these operations in a more robust way (Levy and Fullagar, 1981; Oldenburg et al., 1983; Debeye and Riel, 1990; Robinson and Treitel, 2008).

Our main idea is use deconvolution and integration in one calculation step within the frequency domain. In this case, the result is calculated acoustic impedance with a limited frequency spectrum. Furthermore, the calculation is more stable in the high frequency area and only has problems in low frequencies that may be effectively stabilized based on the Tikhonov and Arsenin (1979) regularization approach.

According to Wiener (1949) deconvolution theory the best results are achieved by knowing the relationship of the power spectrum of noise, to the power spectrum of the result. The power spectrum of noise in many cases can be approximately calculated but the power spectrum of the expected result is

usually unknown. This is the main reason to use Tikhonov and Arsenin's (1979) approach. Also, not only does the seismic signal include error but the wavelet also has its own independent error. This is the second reason to use the approach of Tikhonov and Arsenin.

The method requires only seismic data and wavelet as input; if the wavelet is unknown, it then uses a statistical wavelet. Results can be achieved very quickly because all calculations are done in the frequency domain, based on the Fast Fourier Transform (FFT) technique (Priezzhev, 2010a; Priezzhev, 2010b).

Method

In the extreme case, in which the curve of acoustic impedance can be regarded as continuous and using well-known simplification for reflection coefficients $r_i = (Z_{i+1} - Z_i) / (Z_{i+1} + Z_i) \approx 1/2 \Delta \ln Z$ then a set of reflection coefficients on the trace can be expressed as the differential for the logarithm of impedance $r(t) \approx 1/2 d[\ln Z(t)]/dt$ (Oldenburg et al., 1983), where Z_i, Z_{i+1} are acoustic impedance values for the trace. For the frequency domain, this equation will be $R(\omega) \approx i\omega/2 F[\ln Z(t)]$, where $F[\]$ - is the Fourier transfer operator. Finally, in 1D forward modeling, the equation in the frequency domain based on the convolution equation $S(\omega) = R(\omega)W(\omega)$ will be

$$S(\omega) \approx \frac{i\omega}{2} F[\ln Z(t)] W(\omega) \quad (1)$$

where $S(\omega)$ is the seismic trace spectrum,

$R(\omega)$ is the spectrum of reflectivity coefficients,

$W(\omega)$ is the spectrum of the wavelet,

ω is the given frequency,

$i\omega$ - is the differentiation operator in the frequency domain and $i = \sqrt{-1}$.

The well-known deconvolution equation for seismic trace is based on the Weiner deconvolution (1949):

$$R(\omega) \approx \frac{W(\omega)^* S(\omega)}{|W(\omega)|^2 + \frac{E[N(\omega)N^*(\omega)]}{E[R(\omega)R^*(\omega)]}} \quad (2)$$

where $\frac{E[N(\omega)N^*(\omega)]}{E[R(\omega)R^*(\omega)]}$ is the relation of noise power

spectrums $N(\omega)$ to the power spectrums of the expected result $R(\omega)$.

$E[\]$ is mathematical expectation operator and $*$ a mean complex conjugate.

For deconvolution we can use a constant power spectrum for noise and constant power spectrum for signal because our result is reflection coefficients which have unlimited spectrum with more or less constant power. So usually in equation (2) the noise to signal power spectrum relation function is used like a constant that can prevent division to zero for some frequencies.

In practice, the Weiner equation is not widely used because deconvolution based on sparse signal theory is much more stable and robust (Oldenburg *et al.*,1983; Debeye and Riel, 1990; Robinson and Treitel, 2008).

In order to invert equation (1) to calculate the spectrum of $\ln Z(t)$ we can apply spectrum integration $\frac{1}{iw}$ to (2):

$$F[\ln Z(t)] \approx \frac{2}{iw} \frac{|[W(w)]^* S(w)}{|W(w)|^2 + \alpha M(w)} \quad (3)$$

where $\frac{1}{iw}$ is integration operator in the frequency domain, and

$\alpha M(w)$ is a noise to signal power spectrum relation function based on Weiner theory. But in this case, the expected result is a logarithm of acoustic impedance; this function has not had a constant power spectrum and therefore we cannot use a constant as done in (2). According to Tikhonov and Arsenin (1979), α is a regularization coefficient and $M(w)$ is a regularization operator that must be defined according to prior information; for example, from well log acoustic impedance. If we do not have well data, it can be calculated according to Tikhonov and Arsenin (1979). In common cases, for smooth results it can be $M(w) = w^{2p}$, where p is a constant value > 0 . It is a mean minimization of the stabilization functional

$$\int_{-\infty}^{\infty} M(w) |F[\ln Z(t)]|^2 dw \quad \text{for the convolution equation.}$$

According Tikhonov and Arsenin (1979) this stabilization functional will be very effective if we have instability in high frequency area. In our case we have instability in low frequency area and we propose to use stabilization functional like $M(w) = \frac{1}{w^{2p}}$. This functional is very effective to do

stabilization in frequencies close to 0.

Equation (3) can be used for poststack inversion. It allows calculation of the logarithm of acoustic impedance $\ln Z(t)$ in one step for both deconvolution to calculate reflectivity and integration to calculate the logarithm of acoustic impedance; the result will be calculated using the exponent function $Z(t) = Z_0 e^{\ln Z(t)}$ (Oldenburg *et al.*,1983), where Z_0 is the unknown average level of impedance.

This inversion operator (3) and its spectrum (limited to a frequency band 10-70 Hz) shown on figure 1 looks very similar to the "coloured" inversion operator shown by Lancaster and Whitcombe (2000). Lancaster and Whitcombe derive this operator empirically by comparing an inversion results cube created by conventional technology and a source seismic cube.

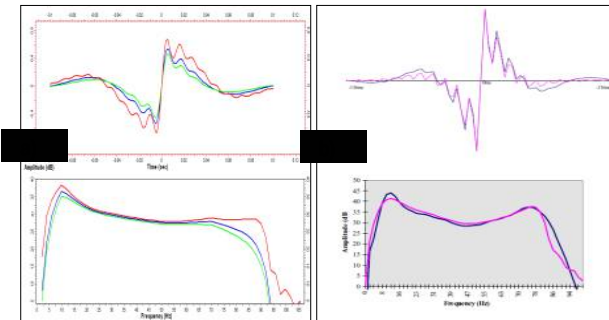


Figure 1. a) - Frequency domain inversion operator and its spectrum (limited for frequency band 10-70Hz) according to different Tikhonov and Arsenin's coefficients (0.01, red; 0.02, blue; 0.03, green). b) - 'coloured' inversion operator and its spectrum (Lancaster and Whitcombe, 2000).

If a Ricker wavelet is used

$$\text{Ricker}(w) = 2/\sqrt{\pi} (ww/w_{\max} w_{\max}) e^{-(w/w_{\max} w_{\max})}$$

then the inversion operator corresponding to this wavelet according (3) will be the following:

$$H(w) = \frac{2}{iw} \frac{1}{\text{Ricker}(w) + a/w^2}$$

where a is Tikhonov and Arsenin's coefficient.

Figure 2 shows an inversion operator and its spectrum for a Ricker wavelet. It is clear to see the low and high frequency parts of this operator. The low frequency part of operator will be stable for close to zero frequencies if use regularization operator $aM(w) = a/w^2$.

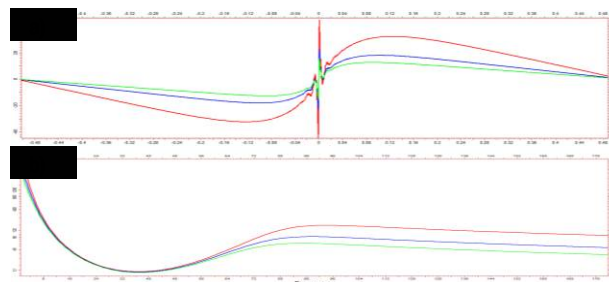


Figure 2. a) inversion operator for Ricker wavelet 30Hz and b) its spectrum (dB) according different Tikhonov and Arsenin's coefficients (0.01, red; 0.02, blue; 0.03, green).

In this case if the wavelet function is unknown and cannot be calculated from seismic and well data, it can be extracted from seismic traces based on the following common simplifications

(Claerbout, 1976; Baan and Pham, 2008; Robinson and Treitel, 2008). The reflectivity function along the trace is a random uncorrelated function. In this case the wavelet autocorrelation and corresponded to it wavelet can be calculated directly from the seismic trace autocorrelation. In frequency domain it will be like the following:

$$E[S(w)S^*(w)] \approx E[W(w)W^*(w)] \quad (4)$$

Finally, based on Wiener deconvolution theory (1949), and Tikhonov and Arsenin (1979) regularization approach, the reflectivity spectrum estimation may be calculated as:

$$R(w) \approx \frac{(E[S(w)S^*(w)])^{\frac{1}{2}} S(w)}{E[S(w)S^*(w)] + \alpha M(w)} \quad (5)$$

Equation (5) may be used as a whitening deconvolution operator with unknown phase shift. Regularization operator can be used for frequency band filtering. Note that the whitening operation can only be used if the wavelet is unknown due to a lot of assumptions (Li *et al.*, 2009).

If combine equations (3) and (5) the whitening inversion will be

$$F[\ln Z(t)] \approx \frac{2}{iw} \frac{(E[S(w)S^*(w)])^{\frac{1}{2}} S(w)}{E[S(w)S^*(w)] + \alpha M(w)} \quad (6)$$

In this case during this operation we use zero phase wavelet $|W(w)| \approx (E[S(w)S^*(w)])^{\frac{1}{2}}$ separate for every trace.

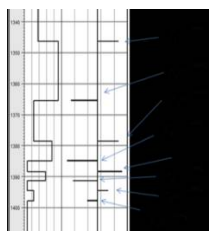


Figure 3. Reflectivity spectrum calculation. Left panel is acoustic impedance model, right panel is reflectivity.

Figure 3 shows the reflectivity spectrum calculation scheme. Every k -th reflection generates the spectrum $r_k e^{-iwt_k}$ and the full reflectivity spectrum will be $R(w) = \sum_{k=1}^K r_k e^{-iwt_k}$ where K is the number of reflections.

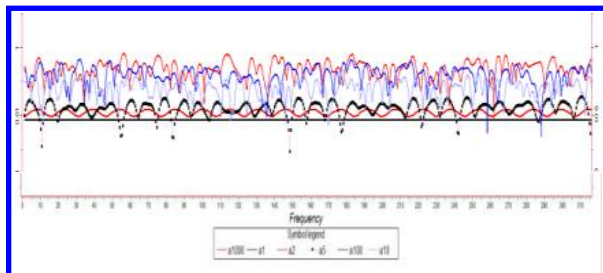


Figure 4. Amplitude (dB) spectrum of reflectivity. Color of curves corresponds to number of reflections. a1 = one reflection, a2 = two reflections, a5 = five reflections, a10 = 10 reflections, a100 = 100 reflections, and a1000 = 1,000 reflections.

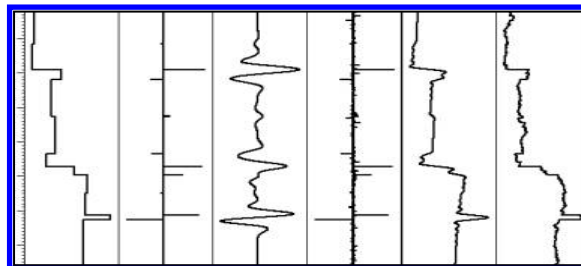


Figure 5. Synthetic modeling and inversion. Panels show (from left to right): first model of acoustic impedance, second reflectivity, third synthetic seismic with Ricker wavelet, fourth deconvolution result using equation (5), fifth inversion result with wavelet equation (3), sixth inversion result based on whitening inversion equation (6).

Figure 4 shows that the reflectivity spectrum is close to a “white” spectrum. So, equation (6) can be used for inversion if the wavelet function is unknown. Figure 5 shows the proposed technology applied to a synthetic dataset and generates similar inversion results both with and without a wavelet.

For prestack inversion the proposed technology is based on the well-known Aki and Richards (2002) equations for PP reflectivity as function of angle:

$$R_{pp}(\theta) = \frac{\Delta Z(\theta)}{Z(\theta)} = C_1 \frac{\Delta V_p}{V_p} + C_2 \frac{\Delta \rho}{\rho} + C_3 \frac{\Delta V_s}{V_s} \quad (7)$$

where $C_1 = 1 + \tan^2 \theta$,

$$C_2 = 1 - 4(\beta/\alpha)^2 \sin^2 \theta$$

$$C_3 = -4(\beta/\alpha)^2 \sin^2 \theta$$

$Z(\theta)$ - elastic impedance (Connolly, 1999) corresponded to angle θ ,

ρ, V_p, V_s - are the density and velocity for P- and S-waves.

If we use a similar simplification to (1), then equation (7) can be rewritten as:

$$\Delta \ln Z(\theta) = C_1 \Delta \ln V_p + C_2 \Delta \ln \rho + C_3 \Delta \ln V_s$$

For the continuous case and if use integration it can be written like $\int_0^t \Delta \ln Z(t) dt = \ln Z(t)$ and according it the equation will be

the following (Hampson and Russell, 2005):

$$\ln Z(\theta) = C_1 \ln V_p + C_2 \ln \rho + C_3 \ln V_s \quad (8)$$

Equation (8) together with (3) or, if the wavelet is unknown (6), can be used for prestack inversion. The calculations can be done in either frequency or time domains.

Examples

Figure 6 shows the seismic whitening results according to (5) and compared with the input data.

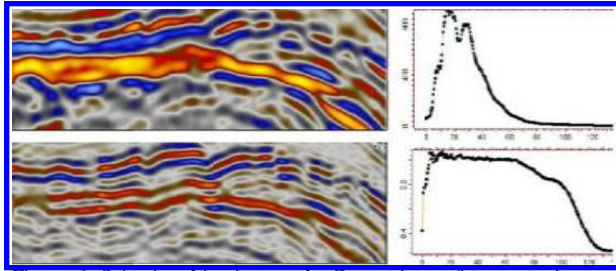


Figure 6. Seismic whitening result. Comparison of cross-section and corresponding spectrum for input data (top row), and same data after whitening operation (bottom row).

A poststack inversion synthetic example is given in Figure 7.

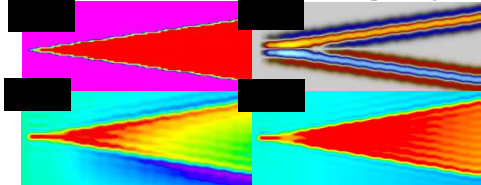


Figure 7. Synthetic example of poststack inversion in a frequency domain. a) Acoustic impedance wedge model. b) Synthetic seismic. c) Inversion result with Tikhonov and Arsenin coefficient 0.1. d) Inversion result with Tikhonov and Arsenin coefficient 0.01.

Figure 8 shows the inversion results based on equation (6), whitening inversion.

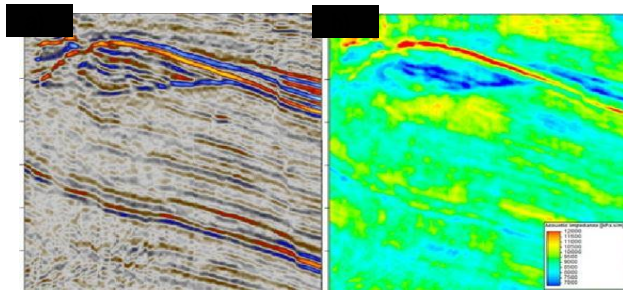


Figure 8. Whitening Inversion result. a) Seismic cross section. b) Acoustic impedance.

Figure 9 shows synthetic examples for prestack inversion based on the proposed technique.

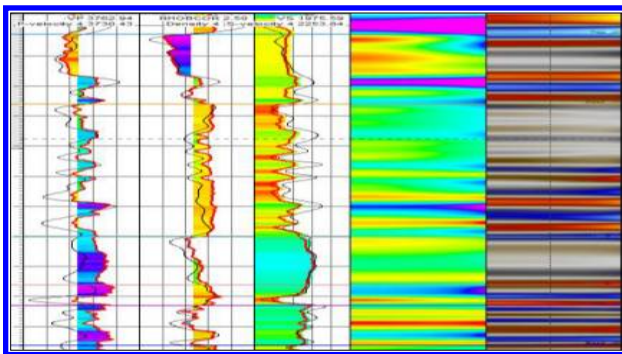


Figure 9. Synthetic example for prestack inversion. On the first three panels the well logs with P-velocity, density and S-velocity are shown.

The colored logs are a source for modeling and the black logs are the inversion results. The fourth panel is forward modeling results; elastic impedance for the angles from 0 to 50 degrees calculated using source P-velocity, density and S-velocity logs using Aki and Richard's (2002) equations. The fifth panel is synthetic seismic for the angles from 0 till 50 degrees calculated using elastic impedance and a Ricker wavelet.

Figure 10 shows prestack inversion results from a real data example. The comparison of the inversion results and independent well log data shows the robustness of the proposed technology.

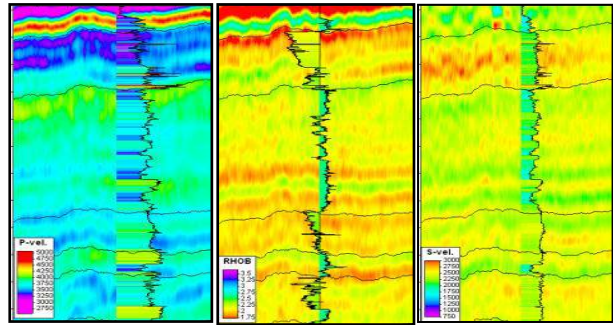


Figure 10. Prestack inversion results on cross sections for P-velocity cube, density cube, and S-velocity cube and their comparison with the well log data corresponded to these cubes.

Conclusions

The proposed technology includes seismic inversion of prestack and poststack seismic data sets with a statistical wavelet or with one extracted from well data. To get stable results we have applied an optimized Wiener filter and Tikhonov and Arsenin's regularization theories. Also, to stabilize the seismic inversion perform the calculations in one step - deconvolution simultaneously with integration. In this case seismic inversion is very stable in high frequency and can be effectively stabilized in low frequency by using stabilization functional $M(w) = \frac{1}{w^{2p}}$. Because in the operation is executed

in the frequency domain, based on the FFT technique, the process is very fast and interactive.

Our fundamental assumption in the proposing this technology is that the minimum use of a prior information will lead to more objective results, independent from the initial approximations introduced by the low frequency models commonly used to stabilize the solutions (Priezzhev *et al.*, 2009; Veeken *et al.*, 2009; Priezzhev, 2010a; Priezzhev, 2010b). This is especially important for applications in exploration.

Acknowledgments

The authors thank Schlumberger for the opportunity to develop this technique and for allowing us to publish the results of the work.

EDITED REFERENCES

Note: This reference list is a copy-edited version of the reference list submitted by the author. Reference lists for the 2012 SEG Technical Program Expanded Abstracts have been copy edited so that references provided with the online metadata for each paper will achieve a high degree of linking to cited sources that appear on the Web.

REFERENCES

- Aki, K., and P. G. Richards, 2002, Quantitative seismology, 2nd ed.: W.H. Freeman and Company.
- Baan, M. V., and D. T. Pham, 2008, Robust wavelet estimation and blind deconvolution of noisy surface seismic: *Geophysics*, **73**, no. 5, 37–46.
- Claerbout, J., 1976, *Fundamentals of seismic data processing*: McGraw-Hill.
- Connolly, P., 1999, Elastic impedance: *The Leading Edge*, **18**, 438–352.
- Debye, H.W.J., and P. V. Riel, 1990, Lp-norm deconvolution: *Geophysical Prospecting*, **38**, 381–403.
- Hampson, D. P., and B. H. Russell, 2005, Simultaneous inversion of pre-stack seismic data: 75th Annual International Meeting, SEG, Expanded Abstracts, 1633–1637.
- Lancaster, S., and D. Whitcombe, 2000, Fast track “colored” inversion: 70th Annual International Meeting, SEG, Expanded Abstracts, 1572–1575.
- Levy, S., and P. K. Fullagar, 1981, Reconstruction of a sparse spike train from a portion of its spectrum and application to high-resolution deconvolution: *Geophysics*, **46**, 1235–1243.
- Li, G., H. Zhou, and C. Zhao, 2009, Potential risks of spectrum whitening deconvolution compared with well-driven deconvolution: *Petroleum Science*, 146–152.
- Oldenburg, D. W., T. Scheuer, and S. Levy, 1983, Recovery of the acoustic impedance from reflection seismograms: *Geophysics*, **48**, 1318–1337.
- Priezzhev, I., L. Shmaryan, and P. Veeken, 2009, Genetic seismic inversion using a nonlinear, multitrace reservoir modeling approach: 71st Annual International Conference and Exhibition, EAGE, Extended Abstracts, P018.
- Priezzhev, I. I., 2010a, Prestack and poststack seismic inversion workflow in frequency domain: 4th Saint Petersburg International Conference, EAGE/EAGO/SEG, Extended Abstracts, B24.
- Priezzhev, I. I., 2010b, Seismic inversion based on angle sums (AVO inversion) in spectral area: *Geoinformatika*, **1**, 64–67.
- Robinson, E. A., S. Treitel, 2008, *Digital imaging and deconvolution: The ABCs of seismic exploration and processing*: SEG.
- Tikhonov, A. N. and V. Y. Arsenin, 1979, *Methods of solving for ill-defined problem*: Moscow Science, 2nd ed.
- Veeken, P.C.H., I. I. Priezzhev, L. E. Shmaryan, Y. I. Shteyn, A. Y. Barkov, and Y. P. Ampilov, 2009, Nonlinear multitrace genetic inversion applied on seismic data across the Shtokman field (offshore northern Russia): *Geophysics*, **74**, no. 6, 49–59.
- Wiener, N., 1949, *The extrapolation, interpolation and smoothing of stationary time series with engineering applications*: Wiley.